Nanostructured PZT Synthesized from Metal–Polyvinyl Alcohol Gel: Studies on Metal–Polymer Interaction

Subir Roy

Defence Metallurgical Research Laboratory, DRDO, Hyderabad 500058, Andhra Pradesh, India

ABSTRACT: $PbZr_{0.53}Ti_{0.47}O_3$ (PZT) nanoparticles of size distribution $\sim$ 1–6 nm were synthesized by single-step autoignition of metal–polyvinyl alcohol (PVA) gel. The physical and chemical bonding between the metals ions and PVA in gel was analyzed from the results of the characterization by FTIR, SEM, and XRD techniques. The appearance of a doublet band between 3500 and 3200 cm^{-1} and the shifting of stretching frequency of O—H band in the FTIR spectra of gel indicated strong electrostatic interaction between the metal ions and the polar OH groups of the polymer. The electrostatic interaction decreased the extent of hydrogen bonding drastically due to engagement of polar OH groups in complex formation with the metal ions. Microstructural study of the dried gel by SEM coupled with its FTIR analyses indicated crosslinking in the metal–polymer gel. The loss of crystallinity of PVA in gel detected by XRD also indicated the drastic degradation of hydrogen bonding in PVA due to the formation of coordination complex with the metal ions. © 2008 Wiley Periodicals, Inc. J Appl Polym Sci 110: 2693–2697, 2008

Key words: lead zirconate titanate; nanoparticle; metal–polymer complex; crosslinking; gel

INTRODUCTION

The applications of polymer in the synthesis of nanoclusters and nanostructured ceramics have been studied by a number of researchers.[1–6] Polymers such as nafion or ethylene methacrylic acid copolymer offer cation exchange sites where cations may be introduced resulting *in situ* precipitation of the compound semiconductors, e.g., CdS and PbS.[1,2] In different applications of polymer, there are examples of the synthesis of CdS, CdSe, and ZnO nanoclusters stabilized by polyvinyl pyrolidone and polyvinyl alcohol (PVA), where the polymers are used as the capping agents and they play an essential role in preventing the flocculation of the concentrated nanoparticles.[3–5] PVA has also been used to produce polycrystalline nanostructured ceramic oxides in which the metal ions (M) interact with the polar —OH groups of PVA to form M-PVA gel followed by the calcination of the gel to produce finally the nanostructured ceramic oxides.[7–9] Recently, auto ignitable M-PVA precursor gel having potential to deliver ultrafine lead lanthanum zirconate titanate (PLZT) particles (1–6 nm) using PVA as the fuel and metal nitrates as the oxidizer has been synthesized in this work by simple adjustment of the polymer/nitrate ratio.[10] The most important characteristic of this synthesis technique is its potential to deliver nanoceramic oxides of particle size range $\sim$ 1–6 nm in the as-ignited powder, with negligible carbonaceous residue (0.6 wt %) and without any additional calcination. Lead zirconate titanate (PZT) and PLZT are the members of the lead-based perovskite family, and are the most studied piezoelectric materials.[11,12] Although reports on the M-PVA gel derived nanostructured ceramic oxides are plenty,[7–9] there are quite a few reports on the detailed investigation into the metal ion–polymer interaction.[13]

In this communication, the author reports the synthesis of PZT by autoignitable M-PVA gel with special reference to the metal ion–polymer bonding interaction based on the results of FTIR, SEM, and XRD analyses of the M-PVA gel.

EXPERIMENTAL

The PZT precursor solutions: mixed oxynitrate solution of $ZrO(NO_3)_2$ and $TiO(NO_3)_2$, was synthesized from the research grade chemicals of $ZrCl_4$, $TiCl_4$. $Pb(NO_3)_2$ solution was obtained from research grade $Pb(NO_3)_2$. These solutions were mixed in the stoichiometric 1.0 : 0.53 : 0.47M ratios to obtain the final precursor solution for $PbZr_{0.53}Ti_{0.47}O_3$. The mixed solution containing stoichiometric amounts of metal ions was reacted with PVA aqueous solution resulting M-PVA sol, followed by evaporation of water to

get M-PVA gel for different nitrate/polymer ratios (R_{np}). The PVA used in this work was obtained in powder form from M/s. s.d. Fine-Chem (Mumbai, India) and has an approximate molecular weight of 14,000 and its degree of saponification is $\sim 90\%$. Extra nitric acid was added to produce different sets of gel with varied nitrate/polymer ratio (R_{np}). The details of the synthesis scheme are same as described in our earlier communication on nano-structured PLZT.[10] The value of R_{np} was varied between 0.28 and 0.56. The degree of auto ignition of the M-PVA gel depended largely on the value of R_{np}. It was observed that gel with R_{np} between 0.45 and 0.53 underwent complete autoignition at $\sim 180^\circ C$ to deliver ceramic powders having negligible carbonaceous residue. The PZT powders were obtained in one-step autoignition of M-PVA gel without any additional calcination of the as-ignited powder. The X-ray diffraction of the powder samples was carried out using a Philips X-ray diffractometer using a Cu kα radiation. The samples for transmission electron microscopy (TEM) observation were prepared by dispersing the powder in methanol and adding a few drops of the suspension on carbon-coated TEM grid. A FEI Tecnai 20G^2 TEM was used for observation. Infrared spectra of all the samples were recorded in KBr medium in the range 4000–400 cm^{-1} with a Perkin–Elmer spectrophotometer. Microstructural study of gold-coated oven dried gel was carried out by scanning electron microscopy (SEM) (LEO-440i). Thermal analysis for the dried gel was carried out using a TG-DTA analyzer (TA Instruments, New Castle, DE, SDT 2960) in air between 30 and 350$^\circ C$, with a heating rate of 10$^\circ C$/min in air.

RESULTS AND DISCUSSION

Structural characterization by XRD and TEM

From the XRD patterns it is observed that the precursor gel with $R_{np} = 0.50$ transforms to rhombohedral PZT along with negligible amounts of PbO (o) and elemental Pb (fcc), after autoignition [Fig. 1(a)]. The presence of unreacted PbO at low temperature is usual in this system, as 100% conversion is not achieved in single-step autoignition. However, the volume percent of unreacted PbO in the as-ignited powder is very low. The appearance of elemental Pb was realized by a single peak of very low intensity and hence its presence was confirmed further by electron diffraction study [Fig. 1(b)]. The presence of fcc Pb was confirmed by calculating the d_{hkl} value from the first four rings and matching the same to that given in the XRD JCPDS data file (JCPDS card no. 01-0972). Formation of elemental Pb is due to the reduction of Pb^{2+} by PVA to some extent. The
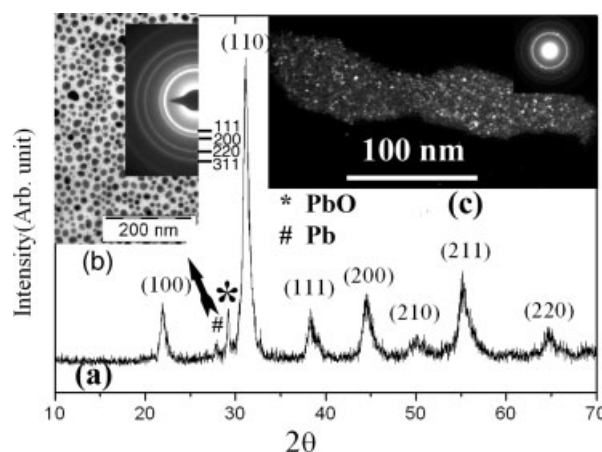

Figure 1 (a) XRD pattern of the as-ignited powder obtained from M-PVA gel with $R_{np} = 0.50$; the inset figures present (b) bright-field TEM image and electron diffraction pattern of elemental Pb (fcc) present as impurity in the as-ignited powder, and (c) dark-field TEM image and the electron diffraction pattern of the PZT nanoparticles in the as-ignited powder.

reducing property of PVA was reported in some recent communications.[14,15] These metallic Pb particles are able to protect themselves from oxidation during autoignition since ignition of gel generates some gases e.g., CO_2, CO which are reducing in nature. Figure 1(c) shows the dark field TEM image of the as-ignited powder obtained from gel with $R_{np} = 0.50$. The particles are spherical, regular shaped with sizes of 1–6 nm. Approximate size distribution of the particles was analyzed manually and it was observed that more than half of the particles in the distribution are within the size range 1–2 nm. Some of the particles are agglomerated having sizes of ~ 4–6 nm. The average particle size is 2.0 nm. The average particle size of the sample was calculated manually by accounting the sizes of 200 particles in the TEM micrograph. The ceramic oxide particles obtained by this method are much finer and assume a narrower size distribution than that obtained in most other techniques.[10] The reason for such particle refinement can be understood from the knowledge of metal ion–polymer interaction in the M-PVA gel.

Chemical reactions

Metal ions–PVA interaction in M-PVA sol/gel

The application of sol-gel chemistry in synthesis of single or multicomponent ceramics oxides offers the opportunity of mixing the component metal ions in molecular level leading to homogeneous sol. The present M-PVA sol-gel is not an example of true organic precursor (alkoxide) based sol-gel synthesis, where metal alkoxides in a sol undergo hydrolysis to form a gel with rigid M-O polymeric network.
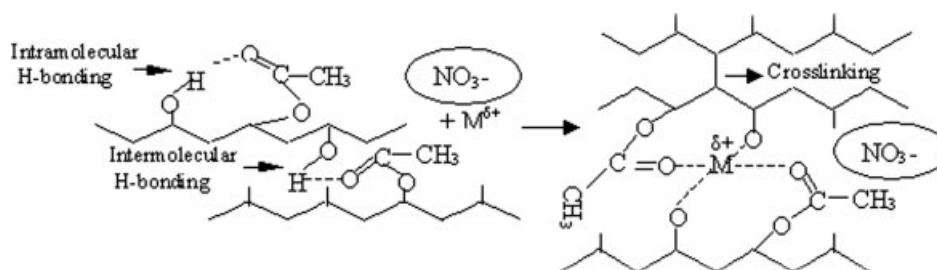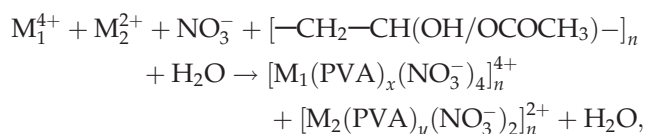
Figure 2 Schematic diagram of chemical reaction between PVA and metal ions.

The M-PVA sol is a product of the reaction between the metal ions and the polymer (PVA). Metal ions added in the form of metal oxy-nitrates react with the polymer via the formation of coordination complex through the polar OH linkages present in the polymer (Fig. 2) and thus help homogeneous distribution of the metal ions. The chemical reaction between the metal ions and the polymer is presented in Figure 2. The schematic diagram of chemical reaction shows that before the addition of the metal ions the OH groups are involved in intramolecular and intermolecular hydrogen bonding with the acetyl C=O groups present on the PVA backbone.[16] In presence of metal ions, both the OH and C=O groups are strongly interacting with the metal ions in coordination complex shown in the diagram (Fig. 2). In dilute condition the reaction product is a very stable sol, which gelled when concentrated by thermal evaporation. The strong interaction between the OH group and the metal ions helps to maintain homogeneous distribution of the metal ions even in gel preventing the segregation of metals.

$$M_1^{4+} + M_2^{2+} + NO_3^- + [-CH_2-CH(OH/OCOCH_3)-]_n$$
$$+ H_2O \rightarrow [M_1(PVA)_x(NO_3^-)_4]_n^{4+}$$
$$+ [M_2(PVA)_y(NO_3^-)_2]_n^{2+} + H_2O,$$

where $M_1 = Ti^{4+}/Zr^{4+}$ and $M_2 = Pb^{2+}$.

Notes: The ligands NO_3^- and PVA satisfy the primary and secondary valences, respectively, of the metal ion in coordination complexes. The value of x and y depends on the coordination number.

Spectroscopic characterization

The bonding interactions between the polymer and the metal ions have been established by the comparison of FTIR spectra of pure polymer (PVA) and M-PVA gel (Fig. 3). In pure PVA, the OH groups are associated by intramolecular and intermolecular hydrogen bonding (Fig. 2). The broad band at $\sim 3000–3550$ cm^{-1} appears due to stretching vibration of the O—H bond.[17,18] The peak broadens due to the association of PVA molecules through strong

H—bonding. The electrostatic interaction between the metal ions and the polymer drastically decreases the extent of H—bonding due to the engagement of polar OH groups and acetyl C=O groups in complex formation with the metal ions. Hence, the band corresponding to the O—H stretching, in the spectrum of M-PVA gel becomes fragmented and relatively sharp. The doublet band appears due to H—bonded O—H stretching (O— H_s^*) and non-H-bonded O—H stretching (O—H_s). Shifting of the O—H_s stretching frequency from $\sim 3600–3650$ cm^{-1} (stretching frequency of non-H-bonded O—H)[15,19] to ~ 3450 cm^{-1} results from the effect of electrostatic interaction involving the OH groups. The band at ~ 1378 cm^{-1} for metal-PVA gel occurs due to O—H in-plane bending vibration (O—H_b), which is not observed for pure PVA, again due to association by H—bonding. The broad band between 1100 and 1000 cm^{-1} in pure PVA appears due to C—O stretching, and is replaced by an intense band in M-PVA gel. This increase in intensity may be assigned as the absorption peak of υ(C—O—C) of the cross-linked PVA.[15] The increase in intensity of the C=O band at 1639 cm^{-1} in M-PVA gel again indicates the involvement of the C=O groups in electrostatic interaction with the metal ions.
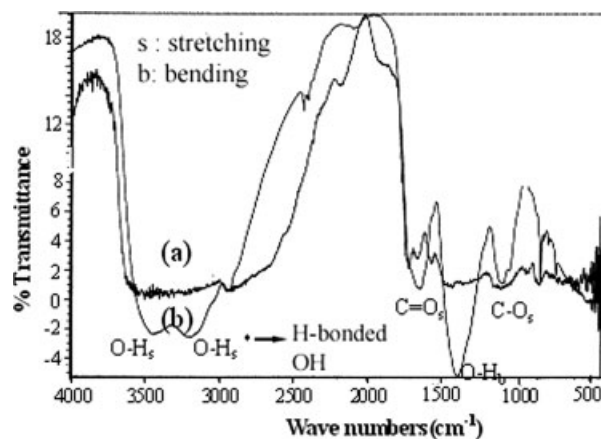

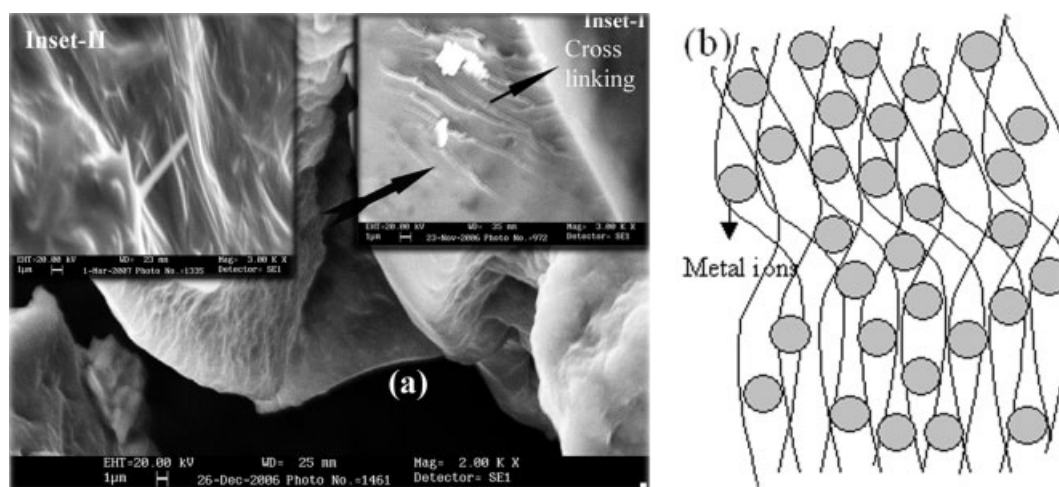**Figure 3** FTIR spectra of (a) pure PVA and (b) M-PVA gel.

Figure 4 (a) SEM micrograph of the oven-dried M-PVA gel showing the crosslinking of the polymer chains in gel; Inset-I: Crosslinked polymer in higher magnification; Inset-II: Micrograph of an isopropoxide-based metal-organic polymeric gel. (b) Schematic diagram of the distribution of metal ions inside the pockets of the crosslinked polymer chains.

Crosslinking of the polymer chains is evident from the SEM micrographs of the oven dried M-PVA gel [Fig. 4(a) and inset-I of Fig. 4(a)]. The assumed distribution of the metal ions inside the pockets of the crosslinked hydrophobic polymer chains is represented by the schematic diagram [Fig. 4(b)]. The chunks of white particles visible in the SEM micrograph are the particles of conducting silver paste used during SEM measurement. The steric hindrance of the hydrophobic polymer chains prevents the metal ions from coming to close proximity and thus minimizes the agglomeration. To compare the microstructure of a M-PVA gel with that of an isopropoxide based metal-organic polymeric gel, the latter was processed using metal-isopropoxide and metal-acetates as the precursors and the dried gel was characterized by SEM. The microstructure is presented in the inset-II of Figure 4(a), which shows polymeric fibers of the gel. The crosslinking is however, absent in the gel reflecting a clear contrast from the microstructure of M-PVA gel. The absence of crosslinking causes agglomeration resulting in larger particle size of the powder synthesized by the isopropoxide precursor based sol-gel method, although the homogeneity in the gel is preserved in the finally synthesized powder.

Crystallinity of the M-PVA gel

The change in crystallinity of PVA in M-PVA gel also indicates strong electrostatic interaction between —OH group and the metal ions. PVA is a semicrystalline polymer. PVA molecular entanglements and crystallinity depend on hydrophilic/hydrophobic force balance. Hydrogen bonding in PVA plays a crucial role in such conformational arrangements, creating hydrophically associated domains.[18] There-

fore, introduction of metal ions in the PVA matrix through coordination complex decreases H-bonding drastically and thus destroys the crystalline structure of PVA. Comparison of XRD results of pure PVA and M-PVA gel reveals that PVA loses its crystallinity by the incorporation of metal ions into its structure due to complex formation [Fig. 5(a,c)]. Moreover, the glass transition temperature of the polymer in gel is also shifted to higher temperature due to complex formation with the metal ions. DTA of the M-PVA gel records its glass transition temperature at 133°C [Fig. 5(d)]. Whereas, the glass transition temperature of pure PVA is 80°C.[20] The commercial PVA used for this experiment is crystalline, having average molecular weight of 14,000. DTA of the same shows melting at 226°C [Fig. 5(d)], which is in accordance with the data reported in literature
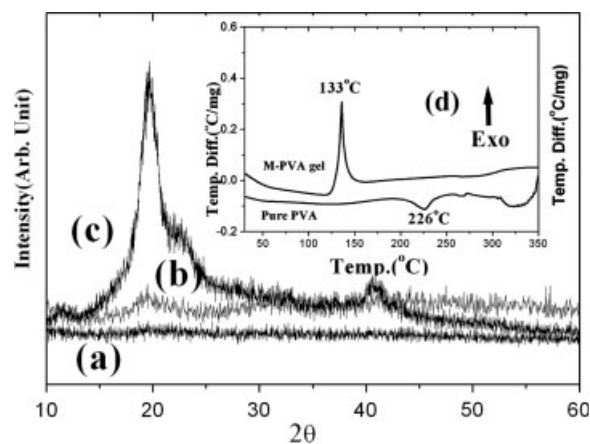

Figure 5 XRD patterns of (a) oven-dried M-PVA gel at 80°C, (b) M-PVA gel annealed at 160°C for 30 min, (c) pure PVA, and (d) DTA curves of pure PVA and oven-dried M-PVA gel (inset).

(225°C).[20] Annealing of M-PVA gel at a temperature (160°C) above its glass transition results in partial recovery of its crystallinity [Fig. 5(b)].

CONCLUSIONS

Spectroscopic characterization of the M-PVA sol, which is a precursor for PZT nanoparticles, showed that both the OH and C=O groups of PVA are strongly interacting with the metal ions forming coordination complex. The strong interaction between the polar OH groups and the metal ions helps to maintain homogeneous distribution of metal ions even in gel, preventing the segregation of metals. The steric hindrance of the hydrophobic polymer chains prevents the metal ions from coming to close proximity and thus minimizes the agglomeration. Introduction of metal ions in the PVA matrix through coordination complex decreases H-bonding drastically and thus destroys the crystalline structure of PVA.

References

1. Mahler, W. Inorg Chem 1988, 27, 435.
2. Hilinski, E.; Lucas, P.; Wang, X. J Chem Phys 1988, 86, 3435.
3. Yao, H.; Takahara, S.; Mizuma, H.; Kozeki, T.; Hayashi, T. Jpn J Appl Phys 1996, 35, 4633.
4. Chevreau, A.; Phillips, B.; Higgins, B. G.; Risbud, S. H. J Mater Chem 1996, 6, 1643.
5. Koch, U.; Fojtik, H.; Weller, H.; Henglein, A. Chem Phys Lett 1985, 122, 507.
6. Roy, S.; Ghose, J. J Magn Magn Mater 2006, 307, 32.
7. Wang, J.; Liu, Q.; Xue, D.; Li, F. J Mater Sci Lett 2002, 21, 1059.
8. Saha, S.; Pramanik, P. Nanostruct Mater 1997, 8, 29.
9. Yamamoto, S.; Kakihana, M.; Kato, S. J Alloys Compd 2000, 297, 81.
10. Roy, S.; Bysakh, S.; Goswami, M. L. N.; Jana, D.; Subrahmanyam, J. Chem Mater 2007, 19, 2622.
11. Roy, S.; Bysakh, S.; Subrahmanyam, J. J Mater Res 2006, 21, 856.
12. Haertling, G. H. Am J Ceram Soc 1999, 82, 797.
13. Morishima, Y.; Fujisawa, K.; Nozakura, S. J Polym Sci: Polym Lett Ed 2003, 163, 141.
14. Luo, L. B.; Yu, S. H.; Qian, H. S.; Zhou, T. Am J Chem Soc 2005, 127, 2822.
15. Gong, J.; Luo, L.; Yu, S.-H.; Qian, H.; Fei, L. J Mater Chem 2006, 16, 101.
16. Bhajantri, R. F.; Ravindrachary, V.; Harisha, A.; Crasta, V.; Nayak, S. P.; Poojary, B. Polymer 2006, 47, 3591.
17. Meyers, R. A., Ed. Interpretation of Infrared Spectra: A Practical Approach, John Coates in Encyclopedia of Analytical Chemistry; Wiley: Chichester, 2000. p 10815.
18. Mansur, H. S.; Oréfice, R. L.; Mansur, A. A. Polymer 2004, 45, 7193.
19. Mansur, H. S.; Oréfice, R. L.; Pereira, M. M.; Lobato, Z. I. P.; Vasconcelos, W. L.; Machado, L. J. C. Spectrosc Int J 2002, 16, 351.
20. Mallapragada, S. K.; Peppas, N. A.; Colombo, P. J Biomed Mater Res 1997, 36, 125.